DOI: 10.1007/s12541-011-0071-2

Manufacturing of Inchworm Robot Using Shape Memory Alloy (SMA) Embedded Composite Structure

Min-Saeng Kim[1], Won-Shik Chu[1,*], Jae-Hoon Lee[1], Yun-Mi Kim[1] and Sung-Hoon Ahn[1,#]

1 School of Mechanical and Aerospace Engineering, Seoul National University, 599 Gwanak-ro, Gwanak-gu, Seoul, Korea, 151-142
* Current Position: Harvard-MIT Division of Health Sciences and Technology, Department of Medicine, Brigham and Women's Hospital, Harvard Medical School, PRB-252, 65 Landsdowne Street, Cambridge, MA, USA, 02139
# Corresponding Author / E-mail: ahnsh@snu.ac.kr, TEL: + 82-2-880-7110, FAX: + 82-2-883-0179

KEYWORDS: Shape memory alloy, Composite, Inchworm, Robot

To design effective movement of robots, various locomotive mechanisms have been investigated. In this study, an inchworm robot was manufactured using shape memory alloy (SMA) which was embedded in composite materials. A Ni-Ti SMA wire was pre-strained and embedded in the glass fiber reinforced polymer (GFRP) strip laid on an ∩-shape mold. Then SMA embedded composite structure was cured at room temperature for 72 hours. Controlling DC current through the SMA wire, the SMA-composite structure, body, could be actuated by changing the radius of curvature. Two legs were attached to the end of body and the leg has two edges which have different coefficients of friction to provide directional movement. One stroke of inchworm provided 4.0 mm translational movement. Repeating on and off of DC current, the inchworm robot gives continuous movement. This mechanism can be applied to the soft morphing robotics, bio medical devices, airplane inlet, etc. instead of using traditional components for their movement.

Manuscript received: July 1, 2010 / Accepted: December 16, 2010

1. Introduction

Shape memory alloys (SMAs) provide functional properties associated with the shape memory effect (SME), which was firstly observed in early 1960s. One of the major advantages of SMAs over other actuator materials is the large recovery force generated by a phase transformation following initial deformation.[1] The generated force per unit area is remarkably high, typically more than 10 times that of traditional electrohydraulic, servomechanical actuators (21–35 MPa), high output exciting actuators for vibration control, and laminated PZT (lead zirconate titanate) actuators (35 MPa).[2] Over the past 10 years, this effect has often been exploited in the form of embedding SMA wire and thin film actuators into a variety of host materials.[3-8] In particular, many clinical biomedical devices have been developed using SMA,[4] including pumps, grippers,[5] and sealing devices.[6]

Recently SMAs were used in many robot actuators because of their high energy density.[7,8] By using an SMA spring as an actuator in a wireless earthworm-like robot, it is possible to mimic the repeated movements of contraction and expansion.[9] Wang *et al.* used SMA wire in rubber/silicone to develop radio frequency-controlled micro fish robot with fin movements resembling those of a squid or cuttlefish.[10] These pioneer researches illustrate various practical applications of the properties of SMA.

In this study, an inchworm robot was fabricated using a SMA embedded in composite material. A wire SMA was embedded into an ∩-shaped glass fiber reinforced polymer (GFRP) strip. The SMA composite inchworm robot was actuated by varying the radius of curvature in accordance with the applied power. This technique is possible to give repeated movement by applying power. To give directional movement, the legs were attached to both ends of robot body with two different friction coefficients. This technique does not need motors or gears which are the traditional components for the moving mechanism, and can be applied to the soft robot actuators, bio medical devices, airplane inlet,[11] etc.

2. Design of the inchworm robot

2.1 Body and legs

Schematic diagram of the inchworm robot with unidirectional movement is shown in Fig. 1. The robot is constructed of GFRP composite, with a single SMA wire embedded in the composite as an actuator. The main body and the actuator are mechanically fastened by bolts and nuts.[11] The synthetic rubber legs are located at

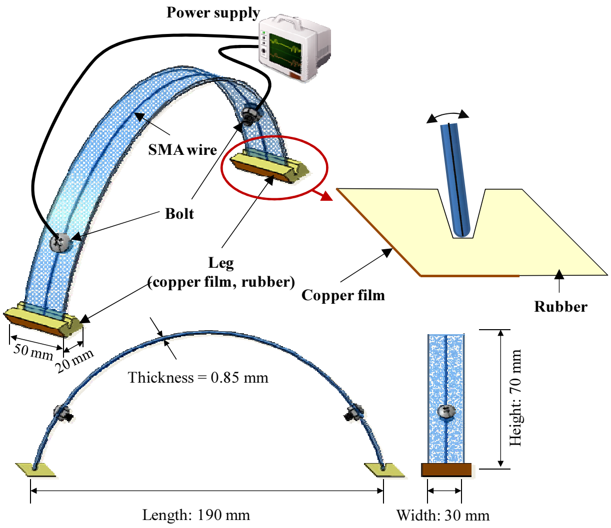

Fig. 1 Schematic diagram of inchworm robot (top) with dimensions (bottom)

both ends of the main body. The length of the robot and height is 190 mm and 75 mm, respectively.

2.2 Motion mechanism

To provide unidirectional movement, the robot has parallelogram-shaped legs shown in Fig. 2 as a cross-section. The synthetic rubber leg has a copper film with a smooth surface (and hence a relatively small coefficient of friction) attached to the front side. F_C and F_R are the friction forces of copper film and of rubber respectively when the forces are applied to the plate of coefficient of friction tester. N is the normal force from total weight (W) of the robot.

The robot body and legs are connected with hinges. After forming the groove on the top surface of the legs, the GFRP composite was inserted into the groove of the leg. The groove was designed to have limited angles of rotation as shown in Fig. 2(a). When the radius of curvature is changed, front or rear leg is designed to be tilted. When the radius of curvature of the body is decreased (contraction), the rear leg is tilted and moves forward (Fig. 2(b)). When radius of curvature is increased (relaxation), the front leg is titled and then the robot body moves forward (Fig. 2(c)). By controlling the radius of curvature of robot body, the robot moves forward step by step.

Fig. 3 illustrates a single motion stroke of the robot. Let δ denote the stroke of the inchworm robot. μ_C and μ_R are the friction coefficients of copper film and rubber, respectively.

2.3 Motion control

When DC power is applied to the SMA wire, the temperature of wire is increased. If the temperature exceeds the phase transformation temperature (PTT), the SMA wire recovers its original length from the pre-strained length. When the temperature is lower than PTT, the SMA wire returns to the pre-strained length. The mechanically fastened GFRP composite structure is controlled by the applied voltage and current of the power supply to SMA wire.

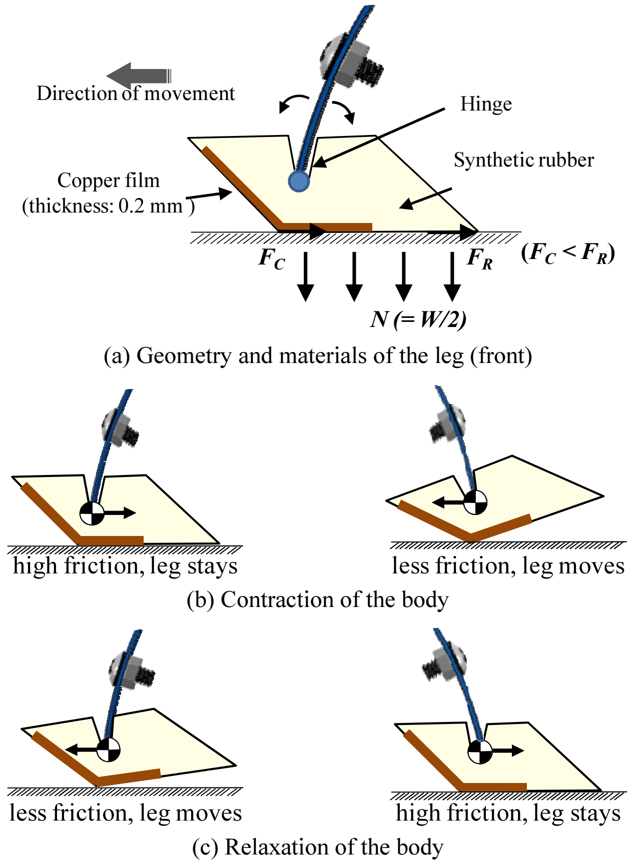

Fig. 2 Schematic diagram of legs and their movement

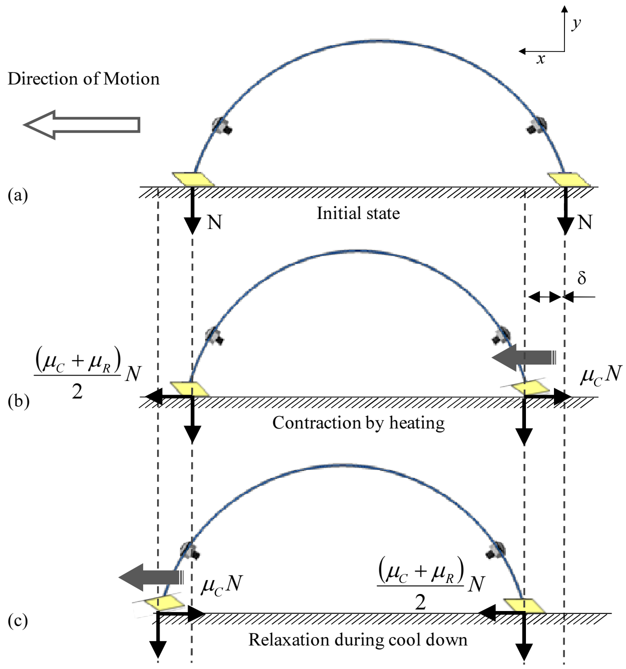

Fig. 3 Motion mechanism of inchworm robot

2.4 Mathematical approach

To predict the motion deflection of the inchworm robot, Castigliano's energy theory was used.[12,13] Since the SMA wire was used as actuator and only gives strain motion, the analysis was simplified and even simplified theory well matches to the experimental data. Because the robot body is symmetric, the center is assumed to be fixed and the force P generated from SMA wire is located the other end. Hence, the deflection in the direction of the x-axis at force P is given by;

$$\delta_x = \frac{\pi P R^3}{4EI} \quad (1)$$

Equation (1) gives the deflection in the direction of the x-axis. R is the radius of curvature of the main body, E is the Young's modulus of the GFRP composite, and I is the moment of inertia which can be calculated from basic moments of inertia equation having rectangular plane area.

3. Fabrication of the inchworm robot

3.1 Materials

Ni-Ti SMA wire has fracture strength of more than 1,300 MPa, and SMA materials are ideal for use in small-size, high output actuators. Ni-Ti SMA wire with a diameter of 0.4 mm and an austenite finish temperature of 80˚C was chosen for this study (Johnson Matthey Co. Ltd., USA). A glass fabric (KN 2100, KPI Co., Ltd., Korea) was used as the host matrix. The thickness of a single layer of the glass fabric was 0.21 mm, and the unit mass was 194 g/m^2. A highly adhesive epoxy resin (YD-128, Kuk-do Chemical Co., Ltd., Korea) with a density of 1.17 g/cm^3 and viscosity of 11,500-13,500 cps (at 25˚C) was used.

The fabrication temperature is an important factor in this research because the shape of the SMA changes by temperature. The YD-128 epoxy resin is a good material for embedding the SMA wire because it cures at room temperature (25˚C), and once it is cured its properties are not changed until the temperature reaches up to 150˚C.

3.2 Fabrication of the robot body

To fabricate an inchworm robot with a given curvature, an ∩-shaped mold is needed. Fig. 4 shows a schematic diagram of the fabrication set up. Using holders and grips, the SMA wire was pre-strained (8% of its original length) and then embedded into the GFRP composite structure.

The main body consisted of three layers of glass fabric and epoxy resin and was cured at 25˚C for 72 hours. Because the SMA wire was the actuator and the robot was ∩-shaped, the wire was located above the bottom layer to take advantage of the eccentric motion. Nuts and bolts were used to mechanically fasten the SMA wire and the GFRP composite together. Fig. 5 shows the fabricated inchworm robot before integrated to the legs.

4. Motion analysis

4.1 Measurement of frictional coefficients

The coefficients of friction of the copper film and the synthetic rubber were measured using an FCMS 170 (Neoplus Ltd., ASTM D 1894). The coefficient of friction of the synthetic rubber (0.80) was 5.3 times higher than that of the copper (0.15) (Fig. 6). Through the mathematical calculation and experiment, these selected materials provide enough difference in coefficient of friction.

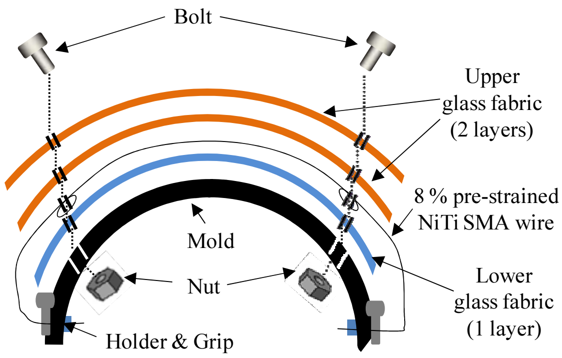

Fig. 4 Schematic diagram of fabrication method

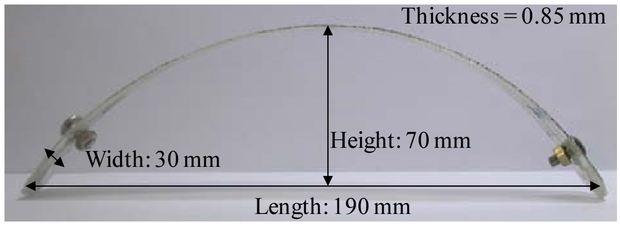

Fig. 5 Fabricated inchworm robot without legs

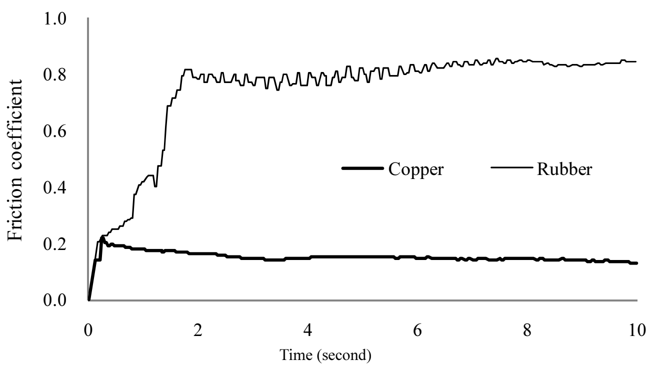

Fig. 6 Coefficients of friction of the copper and synthetic rubber

4.2 Measurement of strain

The deflection of the robot body from the activation of the embedded SMA wires was measured by strain gauges attached to the center of the main body at both top and bottom surfaces. When the temperature of the wire was approximately 90˚C at 3.72 watts (current: 1.38 A, voltage 2.7 V), the strain was 624 μmm/mm at the tension region.

4.3 Thrust force

To calculate the thrust force of the inchworm robot, the weight was measured, as shown in Table 1.

Using the measured coefficients of friction and the weight of each component, the friction force was calculated from equation (2). The minimum thrust force to overcome the friction force was 0.013 N.

$$F_{\min} = \mu_C \left(\frac{W}{2} \right) \quad (2)$$

Table 1 Measured weight of inchworm robot components

Parts	Main body	Leg	Total
Weight (N)	0.097	0.039×2	0.175

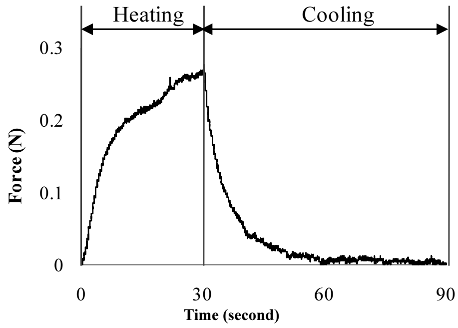

Fig. 7 Generated force of inchworm robot

The generated force was measured with a dynamometer (Type 9256c1, Kistler, Switzerland) and a dSPACE (DS1103 PPC Controller Board, Germany). To perform the experiment, the same power (3.72 watt) was applied as same as used to measure the strain. The signal was analyzed using MATLAB simulink with 200 kHz of sampling frequency and 4 kHz of lowpass filter. Fig. 7 shows the measured force of the robot (0.278 N) over a 90 second interval. A comparison of the calculated and measured values of the working force indicates that the robot is possible to move with the applied power.

The displacement of the robot body can be calculated from equation (1), and taking the friction on the legs into account, a value of 4.47 mm is obtained. Here E is 2.757×10^4 N/mm^2 and I is 1.535×10 mm^4. The experimental (4.42 mm) and calculated values of the displacement are in close agreement.

5. Conclusions

An inchworm robot was manufactured using GFRP composite materials. Ni-Ti SMA wire was used as an actuation module for unidirectional motion. The GFRP composite and SMA wire were mechanically fastened to prevent delamination. The robot body was inserted to the groove of legs which have two different friction coefficients. The robot achieved 4.0 mm of movement over a 90 second interval with 3.72 watts of applied power (relatively low power DC current). And the experiment result and mathematical analysis about the robot movement is well matched.

ACKNOWLEDGEMENT

This research was supported by the Converging Research Center program (No. 2010K001149), Basic Science Research Program (No. 2009-0087640) through the National Research Foundation of Korea (NRF) funded by the Ministry of Education, Science and Technology, and the National Research Foundation of Korea (NRF) grant funded by the Korea government (MEST, No. 2010-0029227).

REFERENCES

1. Shaw, J. A. and Kyriakides, S., "Thermomechanical Aspects of NiTi," Journal of the Mechanics and Physics of Solids, Vol. 43, No. 8, pp. 1243-1281, 1995.
2. Varadan, V. K., Vinoy, K. J. and Gopalakrishnan, S., "Smart Material Systems and MEMS," John Wiley & Sons, Ltd., pp. 63-83, 2006.
3. Wei, Z. G., Sandstrom, R. and Miyazaki, S., "Shape memory materials and hybrid composites for smart systems - Part II Shape-memory hybrid composites," Journal of Materials Science, Vol. 33, No. 15, pp. 3763-3783, 1998.
4. Shahinpoor, M. and Schneider, H.-J., "Intelligent Materials," RSC Publishing, pp. 327-331, 2008.
5. Leo, D. J., "Engineering analysis of Smart materials systems," John Wiley & Sons, Inc, pp. 326-327, 2007.
6. Szweda, R., "Shape memory wire improves sealing of aircraft doors," Sealing Technology, Vol. 2000, No. 78, pp. 7-8, 2000.
7. Reynaerts, D. and Brussel, H. V., "Design aspects of shape memory actuators," Mechatronics, Vol. 8, No. 1, pp. 635-656, 1998.
8. Cho, K. J., Koh, J. S., Kim, S., Chu, W. S., Hong, Y. and Ahn, S. H., "Review of Manufacturing Processes for Soft Biomimetic Robots," Int. J. Precis. Eng. Manuf., Vol. 10, No. 3, pp. 171-181, 2009.
9. Kim, B. K., Lee, M. G., Lee, Y. P., Kim, Y. I. and Lee, G. H., "An earthworm-like micro robot using shape memory alloy actuator," Sensors and Actuators A: Physical, Vol. 125, No. 2, pp. 429-437, 2006.
10. Wang, Z., Hang, G., Li, J., Wang, Y. and Xiao, K., "A micro-robot fish with embedded SMA wire actuated flexible biomimetic fin," Sensors and Actuators A: Physical, Vol. 144, No. 2, pp. 354-360, 2008.
11. Jung, B. S., Kim, M. S., Kim, Y. M., Lee, W. Y. and Ahn, S. H., "Fabrication of a Smart Air Intake Structure using Shape Memory Alloy Wire Embedded Composite," Phys. Scr., Issue T 139, Paper No. 014042, 2010.
12. Beer, F. P., Johnston, E. R., Dewolf, J. T. and Mazurek, D., "Mechanics of Materials, 5th ed.," McGraw-Hill College, pp. 711-719, 2008.
13. Crandall, S. H., Dahl, N. C. and Lardner, T. J., "An Introduction to the Mechanics of Solids, 2nd ed.," McGraw-Hill International Editions, pp. 545-550, 1978.